Synoptics of dust transportation days from Africa toward Italy and central Europe

J. Barkan,[1,2] P. Alpert,[2] H. Kutiel,[1] and P. Kishcha[2]

Received 12 July 2004; revised 12 January 2005; accepted 28 January 2005; published XX Month 2005.

[1] The mean synoptic situation associated with dust outbreaks from the Sahara into the central Mediterranean was examined on a daily basis for the month of July from 1979 to 1992. Composite patterns of wind, geopotential heights, and temperature for dusty days versus those for all days were analyzed. Dusty days were defined as days with the Total Ozone Mapping Spectrometer Aerosol Index (TOMS-AI) in the area around the Apennine peninsula (36°N–46°N, 10°E–18°E) equal to or greater than their monthly average plus 1 standard deviation. It was found that the strength and position of two essential features of the circulation patterns, such as the trough emanating southward from the Icelandic low and the eastern cell of the subtropical high, are the governing factors in making suitable flows for the Saharan dust transportation toward Italy. The deep, well-developed trough near the Atlantic coasts of Europe and Africa, penetrating well to the south, and the strong eastern cell of the subtropical high situated to the northeast from North Africa near the Mediterranean coast, cause strong south-southwestern flows with the potential to carry dust northward into the Mediterranean. In extreme cases the dust can reach Europe north of the Alps and even northern Europe, reaching the shores of the Baltic. These warm flows, accompanied by high dust load, also cause considerable warming in the central Mediterranean region of the order of 6–8 K at 700 hPa. Alternatively, the weak western trough and the weak eastern subtropical cell cause westerlies, which are inconsistent with the Mediterranean dust intrusions. Analysis of the extreme intrusion cases in July 1988, based on TOMS-AI data, and several others in July 2001–2003, based on lidar measurements in Rome, demonstrates the synoptic situation that allows the Saharan dust to reach Italy.

Citation: Barkan, J., P. Alpert, H. Kutiel, and P. Kishcha (2005), Synoptics of dust transportation days from Africa toward Italy and central Europe, *J. Geophys. Res.*, *110*, XXXXXX, doi:10.1029/2004JD005222.

1. Introduction

[2] It is becoming more and more evident, that mineral desert dust particles produce considerable radiative forcing on the climate and influence cloud microphysics [*Kaufman et al.*, 2002; *Prospero et al.*, 2002]. In particular, dust particles scatter and absorb solar and thermal radiation, thus reducing the solar irradiance at the Earth's surface, increasing the solar heating of the atmosphere, and affecting the atmospheric thermal structure. In a cloudy environment, dust enhances the concentration of cloud drops and influences their size, thus changing the potential of clouds to produce rain [*Rosenfeld et al.*, 2002]. Therefore dust significantly affects the synoptic systems. Moreover, dust particles also serve as nutrients to the flora in the Amazon basin and to the sea creatures like algae [*Walsh and Steidinger*, 2001; *Lenes et al.*, 2001; *Swap et al.*, 1992], with important environmental consequences.

[1]Department of Geography, University of Haifa, Haifa, Israel.
[2]Department of Geophysics and Planetary Sciences, Raymond and Beverly Sackler Faculty of Exact Sciences, Tel-Aviv University, Te-Aviv, Israel.

0148-0227/05/2004JD005222$09.00

[3] The African continent, especially its northern part, is one of the main sources of dust around the globe. There are major source areas that emit huge quantities of dust into the atmosphere almost constantly, but more so in the spring and summer months. The most significant sources are in North Africa (North Eastern Algeria, Tunisia and Libya), Mali and Mauritania in West Africa and the Bodele depression near Lake Chad in Central Africa [*Prospero et al.*, 2002; *Washington et al.*, 2000; *Moulin et al.*, 1998; *Barkan et al.*, 2004b]. Strong heating of the Sahara and the Sahel regions in summer causes strong convective disturbances, which elevate huge quantities of dust from the source regions up to the 600–800 hPa levels [*Prospero*, 1996]. The deep warm low, formed because of this heating, causes a strong converging flow, especially from the Northeast, locally called Harmattan. This flow adds to the already existing dust by uprooting dust particles and lifting them up [*Karayampudi et al.*, 1999]. Consequently, the atmosphere above North Africa is loaded with dust, available for transport according to the prevailing flow [*Israelevich et al.*, 2002]. The bulk of the dust is transported westward into the Atlantic Ocean [*Barkan et al.*, 2004a] and southward

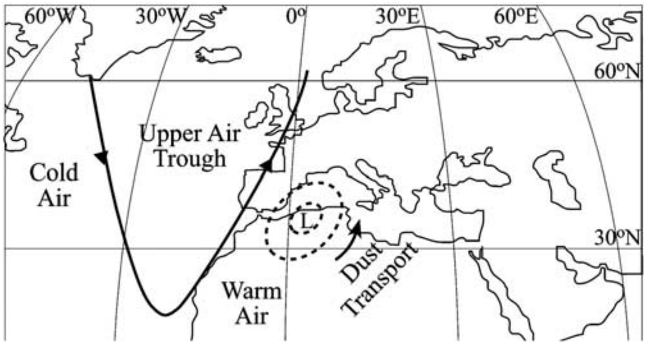

Figure 1. Schematic map of the general synoptic situation in periods of dust outbreaks from the Sahara into Europe: solid line, 700 hPa; dashed line, surface.

with the strong northerlies prevailing in the summer months. However, a not negligible part, estimated as 80–120 Tg per year, transported northward across the Mediterranean into southern and even central Europe [*Collaud Coen et al.*, 2003; *Dulac et al.*, 1996].

[4] There is a marked difference between the vertical structure of the elevated dust layers over the Atlantic and over the Mediterranean. While the plumes over the Atlantic are quite similar from outbreak to outbreak, the structure of the plumes over the Mediterranean is erratic and changes from case to case [*Koren et al.*, 2003]. According to lidar observations, the dust transported toward and over the Mediterranean is located in distinct layers separated by clear air, between 1.5 and 5 km [*Hamonou et al.*, 1999]. According to *Collaud Coen et al.* [2003], in their work on Saharan dust events at the Jungfraujoch, the transportation to Europe north of the Alps occurs at higher levels, between 2.5 and 6.5 km. Other lidar observations of Saharan dust, carried out at the island of Lampedusa in the Mediterranean, detected large dust concentrations up to 7 or 8 km in altitude lasting a few days [*Di Sarra et al.*, 2001]. During strong perturbations dust can reach up to 10 km in altitude and may last there for several days [*Gobbi et al.*, 2000]. A climatological analysis of 3-D dust distributions by *Alpert et al.* [2004], based on 2.5 year archive of 48 h dust forecast over the whole Sahara and vicinity regions, revealed results consistent with lidar observations. On average, dust over the Atlantic penetrates up to $\leq$5 km while over the Mediterranean up to $\leq$8 km. According to *Alpert et al.* [2004], the characteristic feature of dust vertical profiles over the main Saharan dust sources is its maximal concentration near the surface.

[5] The origin of the dust transported across the Mediterranean and into Europe is mainly from the northern dust sources, that is, Tunisia, Algeria and Libya [*Prodi and Fea*, 1979; *Avila et al.*, 1996; *Bonelli and Marcazzan*, 1996], but more southern and western sources cannot be excluded. During these outbreaks, huge fanlike dust plumes invade the Mediterranean and occasionally cross into south Europe and can reach the Alpine region and central Europe [*Collaud Coen et al.*, 2003, *Alpert and Ganor*, 1993, *Prodi and Fea*, 1979]. These plumes can start out from many small discrete sources and spread out around the main source areas. Narrow plumes from these secondary sources merge downwind, eventually becoming the huge plumes mentioned above [*Koren et al.*, 2003].

[6] The transportation of the Saharan dust toward Europe is caused by intense cyclones that pass the North African coast of the Mediterranean from west to east. Deep north south oriented troughs in the upper layers of the atmosphere transport cold air from the high latitudes into North Africa (Figure 1). Along the front between this cold air and the warm African air, deep lows are formed. Around these lows the horizontal wind flow is very strong (10 s of m s^{-1}) and the vertical flow caused by the convective forces is also of considerable strength. The joint effect of these two flows causes uplifting of the dust and its transportation over long distances. These lows move eastward together with the upper air troughs. The strong southwestern flow, in the eastern-forward flank of the lows, transports the dust toward central Europe [*Prodi and Fea*, 1979; *Moulin et al.*, 1998; *Dayan et al.*, 1991; *Conte et al.*, 1996; *Bonelli and Marcazzan*, 1996; *Collaud Coen et al.*, 2003].

[7] The peak of the dust activity is in spring and summer [*Dulac et al.*, 1996]. In spring the main dust activity is observed in the eastern Mediterranean due to the warm (sharav) lows moving along the African coast from west to east [*Alpert and Ziv*, 1989; *Egger et al.*, 1995]. In the summer months the maximum of dust activity moves westward into the central Mediterranean, while toward the end of the summer months it moves to the Western Mediterranean [*Moulin et al.*, 1998].

[8] The present study is aimed at defining the mean synoptic situation in such events, especially in cases of dust transportation over the Italian peninsula. Understanding the synoptic situation may help to improve the dust packages in atmospheric models. The understanding and describing of the synoptic situation can help in predicting dust generation, with application to a wide range of topics like traffic safety, agriculture, marine biology, health problems, etc. In addition, a better understanding of the synoptics associated with deep dust intrusion may help the forecasters to improve their predictions.

2. Methodology and Data Processing

[9] This work is based on data for the months of July from 1979 to 1992. July is typified with the highest dust activity in the central and western Mediterranean. The months of May and June were also inspected (not shown). These months were just as dusty as the month of July and the dust transport conditions were basically the same as those described in the current study.

[10] The Total Ozone Mapping Spectrometer aerosol index (AI) daily data were used to estimate the total dust amount [*Herman and Celarier*, 1997]. This index utilized the spectral contrast of two ultraviolet channels: 340 nm and 380 nm. It is positive for dust and proportional to the amount of the aerosol in the column along the line of sight. The TOMS AI index is an effective measure for dust mainly at altitudes higher than 1 km, and was proven to be effective in improving dust initialization for dust prediction models [*Alpert et al.*, 2004]. As far as the reliability of the AI calculation below 1 km is concerned, *Herman and Celarier* [1997] found that UV-absorbing aerosols in the boundary layer near the ground could not readily be detected by the

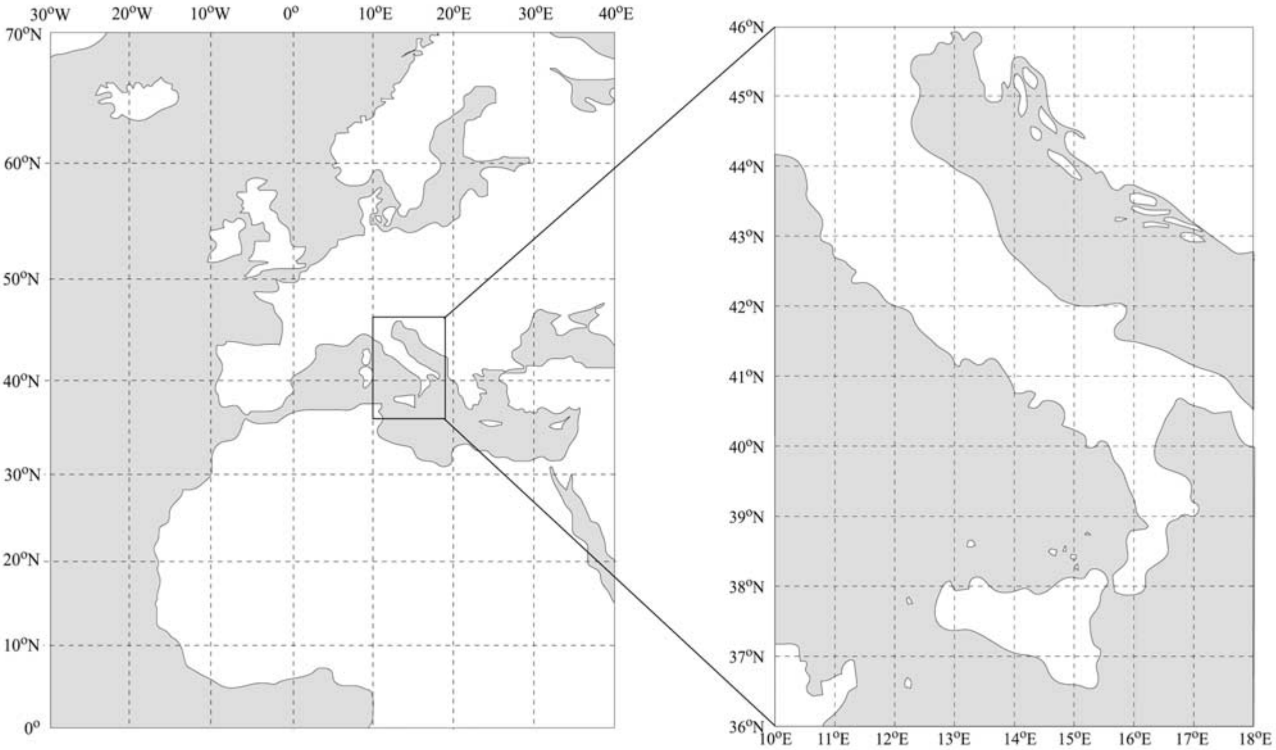

Figure 2. (a) NCEP/NCAR data acquisition area. (b) Aerosol index acquisition area.

method used for AI calculation. The cause was that near the ground the signal was relatively weak to the apparent noise from the ground. It means that the accuracy of AI is not enough below 1 km while above 1 km it is better. At the same time, *Torres et al.* [2002] consider that for mineral dust this restriction for TOMS AI is not so important and AI allows detection of dust particles even close to the ground. The great advantage of the TOMS AI is, that due to the very low albedo of the UV particularly above land, it is able to measure dust everywhere above land and sea [*Prospero et al.*, 2002]. It is the only dust-measuring instrument with this kind of capability, which has been operating since 1979.

[11] The daily data of the wind components, geopotential heights and temperature at the 700 hPa level were obtained from the National Centers for Environmental Protection/National Center for Atmospheric Research (NCEP/NCAR) reanalysis project. The 700 hPa level was chosen because the average transportation of the dust takes place above the humid trade wind air of the PBL, between 600–800 hPa [*Carlson and Prospero*, 1972; *Prospero*, 1996; *Hamonou et al.*, 1999; *Alpert et al.*, 2004; *Westphal et al.*, 1987]. The AI data for the present study cover the area 36°N–46°N, 10°E–18°E, with resolution of 1° latitude and 1.25° longitude. The NCEP/NCAR data for the synoptic analysis was taken from the area 0°–70°N, 40°W–40°E, with resolution of 2.5° latitude and 2.5° longitude (Figure 2).

[12] The daily Total Ozone Mapping Spectrometer Aerosol Index (TOMS-AI) values were standardized for each year in the period 1979–1992. Doing so we reduce the mean of series to 0 and its standard deviation to 1.

$$Z = (AI - AI_{mean})/\sigma AI \quad (1)$$

The obtained values of the standardized AI are dimensionless. Negative standard scores indicate below average values, whereas positive scores, above average values. all the dusty periods for Italy were identified according to this definition.

[13] Table 1 presents 43 dusty days out of a total number of 341 analyzed days. Therefore about 12% of the July days were classified as ''dusty''. Every dusty day was counted separately regardless if it was a single or part of several consecutive days. It is worth noting that this separation between dusty and nondusty days is somewhat arbitrary. Nevertheless, our estimate is quantitatively supported by lidar soundings over Rome. *Kishcha et al.* [2004] reported about 18 dusty days (out of 93 days) for the three Julys of 2001–2003, which are about 19% of the days over that 3 year period. The AERONET stations of Rome and Oristano verified the dusty character of these days. The

Table 1. Days with $Z \geq 1.0$: July 1979–1992[a]

Year	Dates
1979	21
1981	1, 2, 3, 9
1982	6, 15, 16, 30, 31
1983	20, 21, 22, 25, 26, 27, 28, 29, 30
1984	1, 2, 4, 12, 25, 26
1985	3, 4, 16
1986	7, 24, 26
1987	20, 23, 24
1988	1, 5, 6, 7, 8, 9, 20
1989	6
1990	1

[a]Total number of all cases: 341. Total number of dusty cases ($Z \geq 1.0$): 43. Average AI: 0.45. Standard deviation: 0.44. Average plus standard deviation: 0.89.

Table 2. Aerosol Index as Function of the Wind Direction, Italy, for the Month of July, 1979–1992

Wind Direction Sector, deg.	Mean Aerosol Index
0–45	0.33
45–90	0.24
90–135	0.27
135–180	1.26
180–225	1.07
225–270	0.8
270–315	0.83
315–360	0.58

AOT measured in these days were well above average, while the AOT in days not defined by the lidar as dusty were below the average. The fact that in the lidar measurements 19% of the days defined as dusty while with the statistical method we employed 12% were defined as dusty, confirms that this statistical methodology is rigorous and that only really dusty days are included in the research.

[14] According to the above definition, all the dusty periods for Italy were identified (Table 1). Average 700 hPa maps of wind flow, geopotential height and temperature, for all the days, dusty days and the difference between them, were prepared.

[15] The average AI value for every 45° sector was calculated (section 3.4 and Table 2). In order to validate the NCEP/NCAR database we prepared wind flow maps also using the ECMWF database (Figures 3a, 3b, and 3c). No significant differences were found.

[16] We analyzed a case study for the outstandingly dusty period of 5–9 July 1988. The obtained results were very similar to these of the general cases. In an additional case study we examined the transportation of the dust to central Europe in 27–28 July 1983. The synoptic situation in dusty cases identified by lidar measurements in Rome Italy in the years 2001–2003 was compared with the synoptics in the research period and found almost identical.

3. Results and Discussion

3.1. Wind Flow

[17] Figure 3a shows the mean wind flow for all the July months of the research period (1979–1992) at the 700 hPa level. Two separate cells of the subtropical high are visible. One in the Saharan region its center approximately at 32°N–5°E. The other is in the middle Atlantic but its center is out of the research area. Between them is a weak trough situated along the western coast of Africa, terminated at 30°N. Around the Saharan high is quite a strong flow, westerly at its northern flank in particular over the Italian peninsula. The flow in its western flank is southwesterly, but because of the westerly location of the high the stronger part of this flow is over the Atlantic and obviously does not lift and carry dust. In the northern side of the high, the flow, though westerly, turns southward west of the Italian peninsula, and is not well situated to deposit dust in the peninsula even if the dust was available. Between latitudes 45°N–60°N the flow is an undisturbed westerly.

[18] The mean flow during the dusty episodes is shown in Figure 3b. The two high-pressure cells exist like in the mean conditions (Figure 3a) but definitely stronger. The Saharan cell is located somewhat to the east and north relative to the

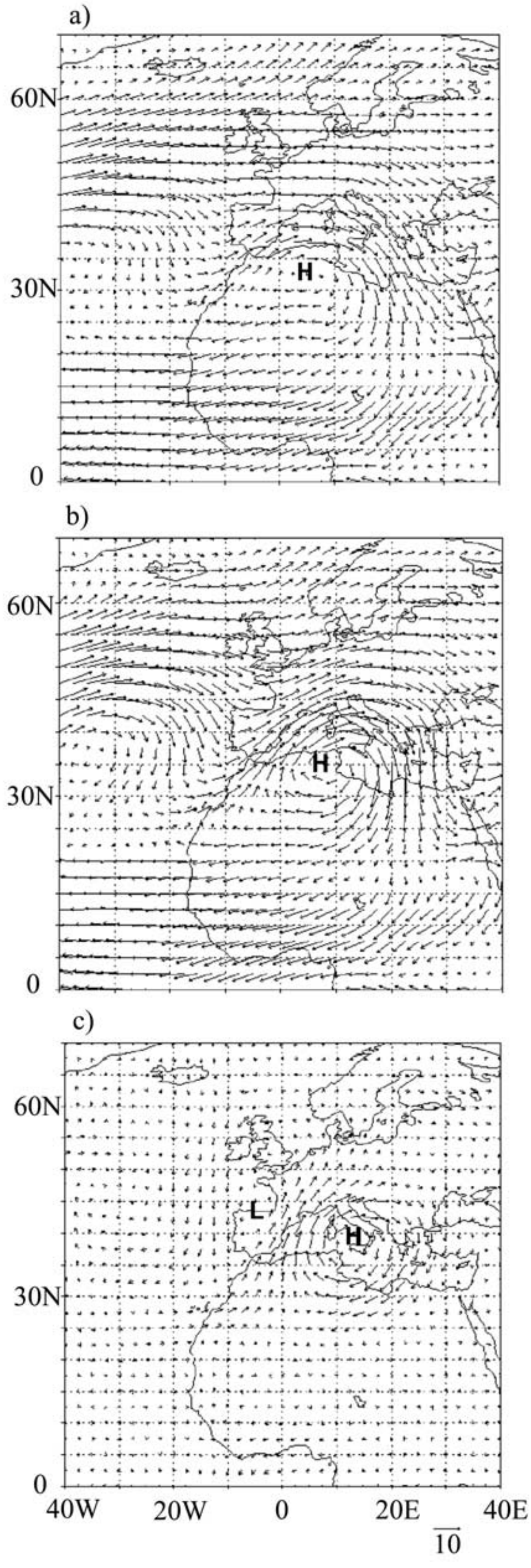

Figure 3. (a) Average wind flow of all the cases at 700 hPa for the month of July (1979–1992). (b) Average wind flow of the dusty cases at 700 hPa for the month of July (1979–1992). (c) Average wind flow difference, that is, dusty cases minus all the cases over the study region, for the month of July (1979–1992).

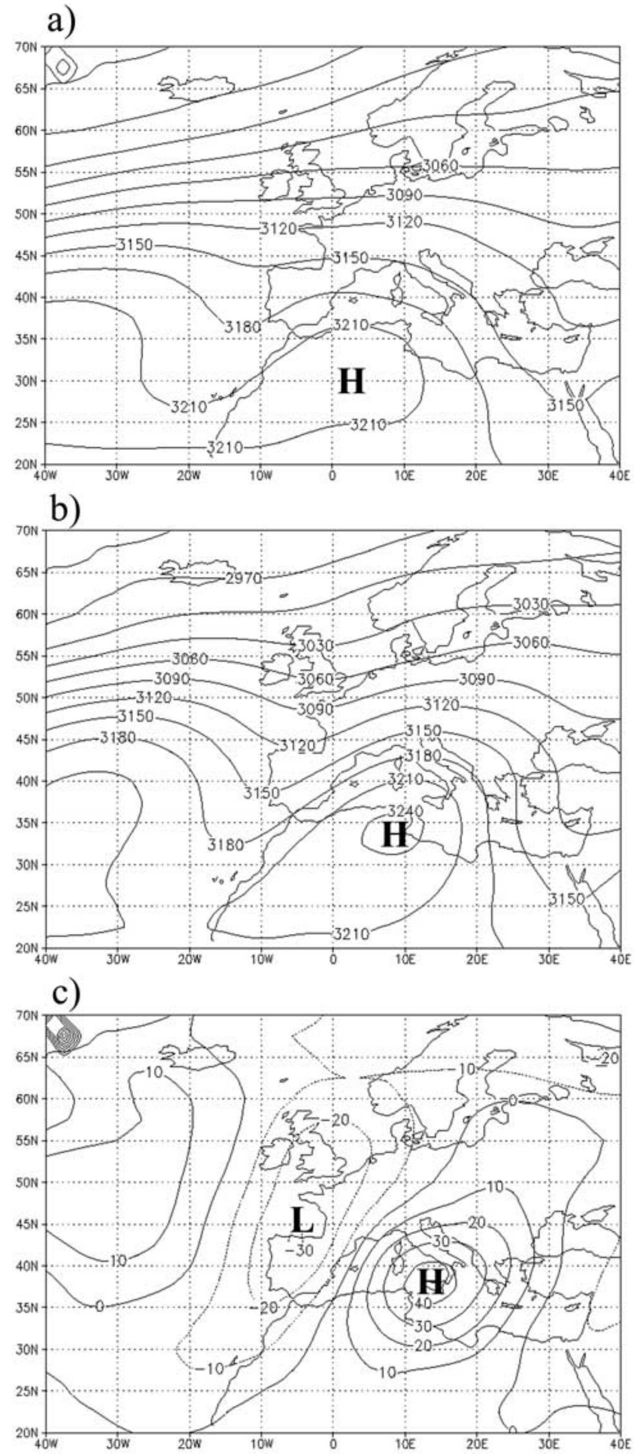

Figure 4. (a) Average geopotential height of all the cases at 700 hPa, July 1979–1992. (b) Average geopotential height of the dusty cases at 700 hPa, July 1979–1992. (c) Average geopotential height difference, dusty cases minus all cases, July 1979–1992.

mean conditions (at approximately 35°N–10°E). The Atlantic cell moved more to the east. Its center can be seen in the research area at 35°N–35°W. Between the two cells the trough is considerably stronger and exists between latitudes 27°N–47°N. The flow between this deep trough and the Saharan high is strong southwesterly toward the central Mediterranean and the Italian peninsula. Due to the more easterly location of the high the stronger part of the flow passes over the dust source areas of Mauritania and Mali [*Prospero et al.*, 2002; *Barkan et al.*, 2004b] and presumably picks up great amount of dust and carries it toward Italy.

[19] Following *Stidd* [1956], the anomaly of wind flow for dusty cases from the normal conditions was analyzed in order to understand the difference (Figure 3c). The greatest differences can be observed over the central Mediterranean causing an intensification of southeasterly flow toward Italy. A trough, parallel and close to the African coast, emanating from it till latitude 27N. The flow in the African side of the high can bring dust not only from the western sources but also from the ones situated more to the east, and deposit it in Italy and even in the other side of the Adriatic.

[20] The question arises, however, why the flow in the actual dusty days is analyzed while the process of the transportation of the dust could begin several days earlier? *Israelevich et al.* [2002] stated that there is a perpetual reservoir of dust in the Saharan atmosphere. When a suitable flow is formed the dust is immediately available for transportation from every point along the path even from points several hours away from the research area.

3.2. Geopotential Height

[21] To obtain an additional view of the synoptic variation, the composite patterns of geopotential height at 700 hPa level were analyzed in the same manner as for the wind flow. Figure 4a displays the mean isohypses for July. The Saharan high is quite weak; its center is in the same location as in Figure 3a. The 3210 m isohyps barely touches the African continent on the high's west side and turns sharply southward on its east side. The 3180 m isohyps passes south of Italy and turns southward near Sicily. The trough west of Africa is weak, its northern edge at the northwestern tip of the Iberian Peninsula and in the south it terminates at the vicinity of the Canary Islands with very weak gradients.

[22] The mean isohypses for the dusty cases are shown in Figure 4b. Compared to the normal conditions, the Saharan high is stronger and located considerably farther east and northward touching the Gulf of Gabes (33°N, 11°E). Its center value is over 3240 m. The trough west of the African coast is deeper also and can be identified as far north as England. The most important feature though is the steep, southwesterly gradient, between the trough and the Saharan high along the Western Sahara and the western Mediterranean basin.

[23] The difference map between the mean of the dusty cases and the mean of all the cases (Figure 4c) shows a closed high with 40 m with positive difference at its center around Sicily. A closed low with a −30 m difference at its center over northern Spain is located west of the abovementioned high. Between these two systems there is a steep gradient, south southwesterly in North Africa and over the western Mediterranean and westerly in the central Mediterranean toward Italy.

3.3. Temperature

[24] The temperature at 700 hPa was examined in the same way as the wind flow and the geopotential height

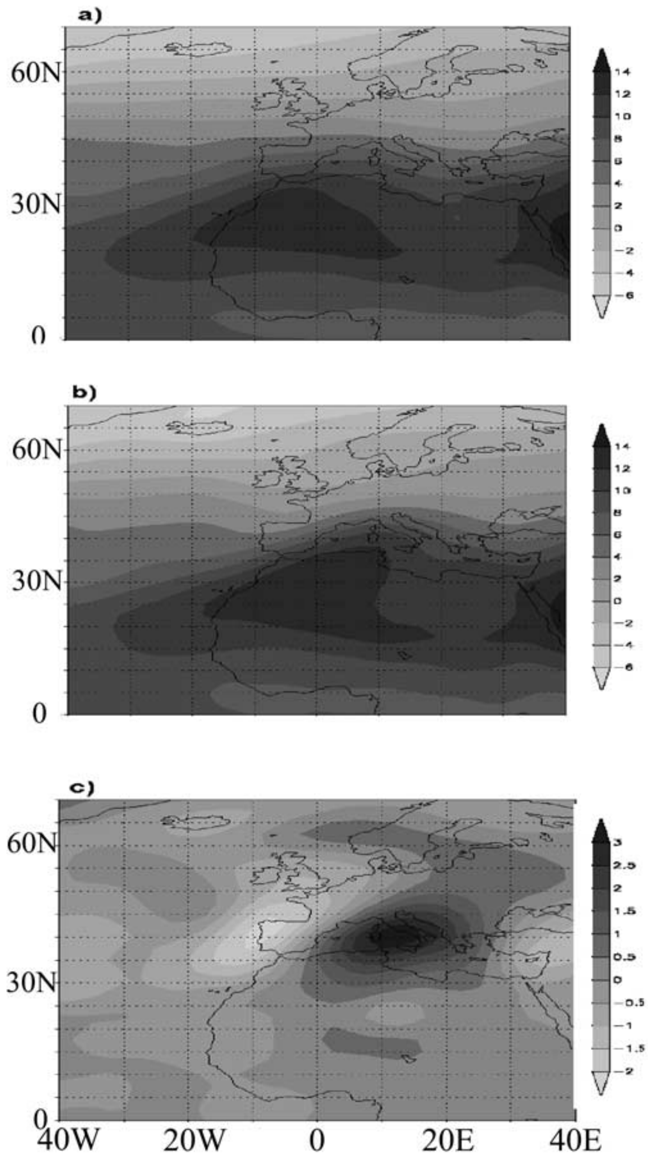

Figure 5. (a) Average temperature of all the cases at 700 hPa, July 1979–1992. (b) Average temperature of the dusty cases at 700 hPa, July 1979–1992. (c) Average temperature difference, dusty cases minus all cases, July 1979–1992.

above. As mentioned in section 2, the 700 hPa level was chosen because the bulk of the dust transportation happens in this level. In Figure 5a the spatial distribution of the mean temperature in July is shown. The hottest area is in the western Saharan region. Away from this area the temperature cools uniformly as a function of latitude, northward and southward.

[25] Figure 5b shows the temperature at the 700 hPa level for the dusty episodes. It is important to notice that a warm tongue emanating from the hot kernel, shown in Figure 5a, northeastward toward the central Mediterranean and Italy.

[26] Figure 5c shows the differences between the mean dusty conditions and the normal for all July days. Positive differences of greater than 3°C are seen over the Italian peninsula. Although the warm southwesterly flow toward Italy in the dusty cases is perhaps the main reason to this phenomenon, we believe that to the presence of large amounts of dust in the atmosphere above Italy has also a contribution to this temperature increase [*Alpert et al.*, 1998].

3.4. Distribution of the Dust by the Wind Direction

[27] To identify the areas that contribute most of the dust to central Europe, we computed the mean AI as function of the wind direction in the area 10°E–14°E, 42°N–44°N, by sectors of 45° (Table 2). It can be seen that the main directions providing the dust to Italy are between southeast (135°) and southwest (225°) while the sector between southwest and northwest (315°) is slightly less dusty. There is no dust supply from the easterly and north directions, which is reasonable considering the mean flow in the dusty events.

3.5. Case Studies

3.5.1. Five Consecutive Dusty Days

[28] A case of five days of great quantity of dust in the atmosphere above Italy, between 5–9 July 1988 was investigated. This period of successive dusty days was chosen because of the high values of AI in it, although there were other even longer dusty periods (Table 1) but with lower AI values.

[29] Figure 6 shows the distribution of the mean AI values around Italy for these days. It can be seen that the bulk of the dust was transported from the south and the southwest toward central and northern Italy where the AI values were from 2.4 up. In southern Italy the dust coverage was lighter but even there the AI was 1.5–1.8 which is considerably above the normal conditions.

[30] Compared with the mean July flow (Figure 3a) the mean flow of these five days (Figure 7a) is markedly

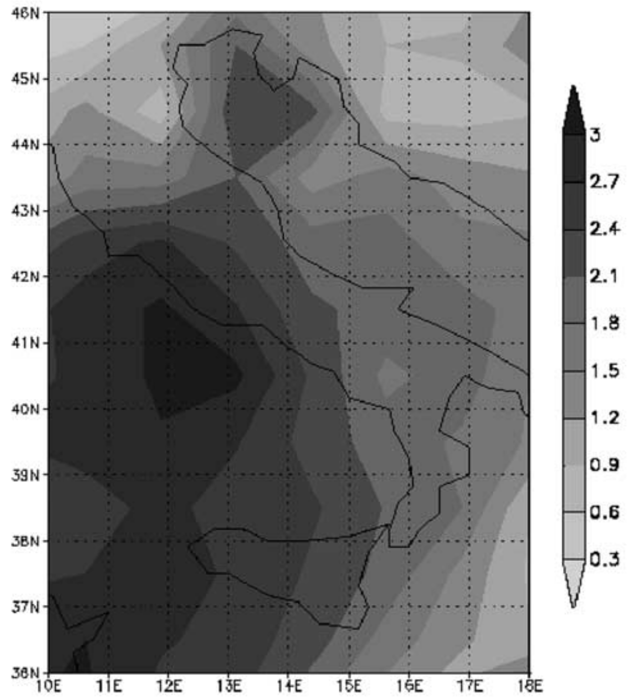

Figure 6. Average aerosol index for 5–9 July 1988 in Italy and vicinity.

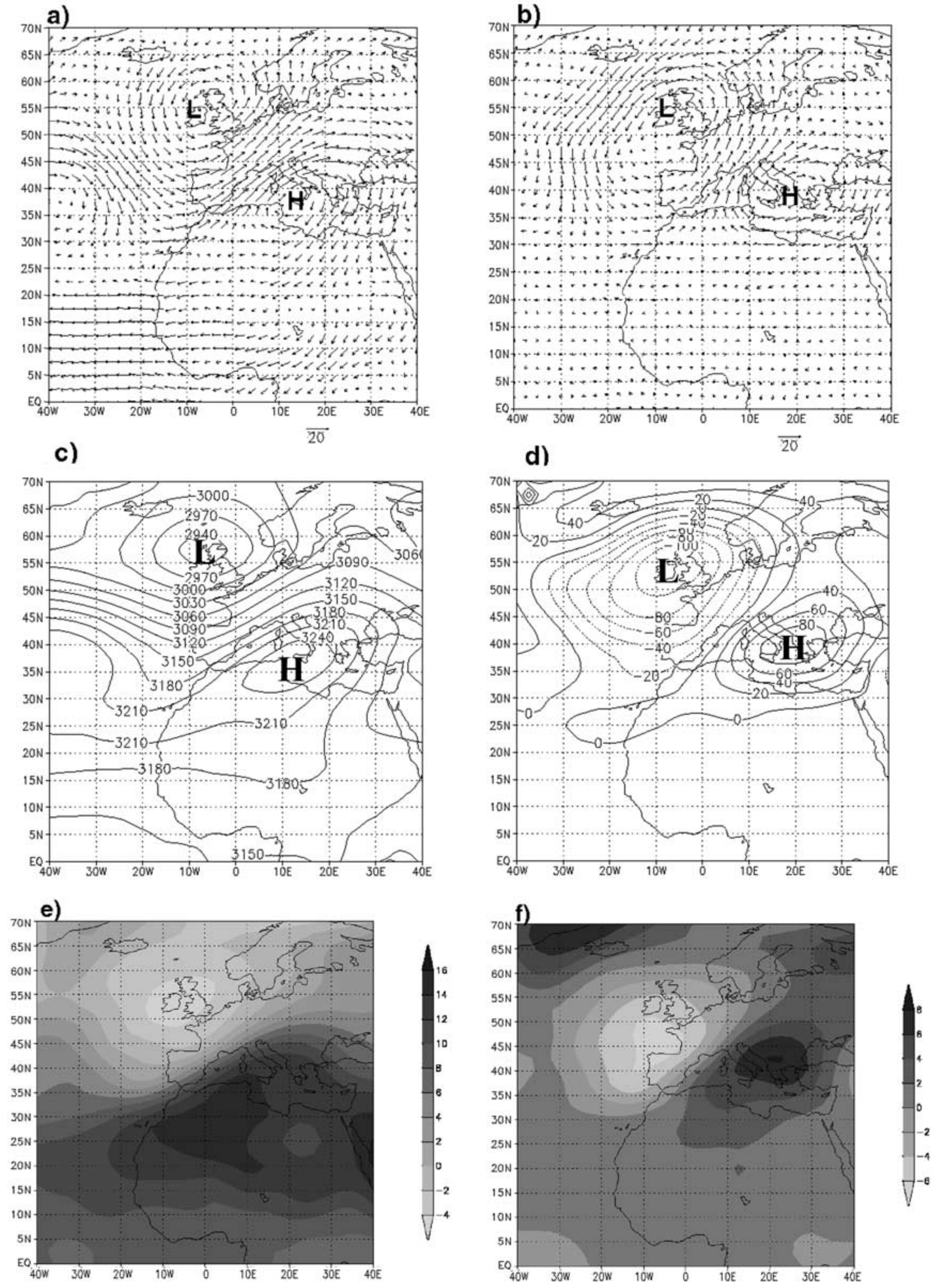

Figure 7. (a) Average wind flow of the dusty period 5–9 July 1988 at 700 hPa. (b) Wind flow differences between the averaged wind distribution during the dusty period 5–9 July 1988 and the one for all the cases. (c) Average geopotential height of the dusty period 5–9 July 1988 at 700 hPa. (d) Geopotential height differences between the averaged distribution of geopotential height during the dusty period 5–9 July 1988 and the one for all the cases. (e) Average temperature of the dusty period 5–9 July 1988 at 700 hPa. (f) Temperature differences between the averaged distribution of temperature during the dusty period 5–9 July 1988 and the one for all the cases.

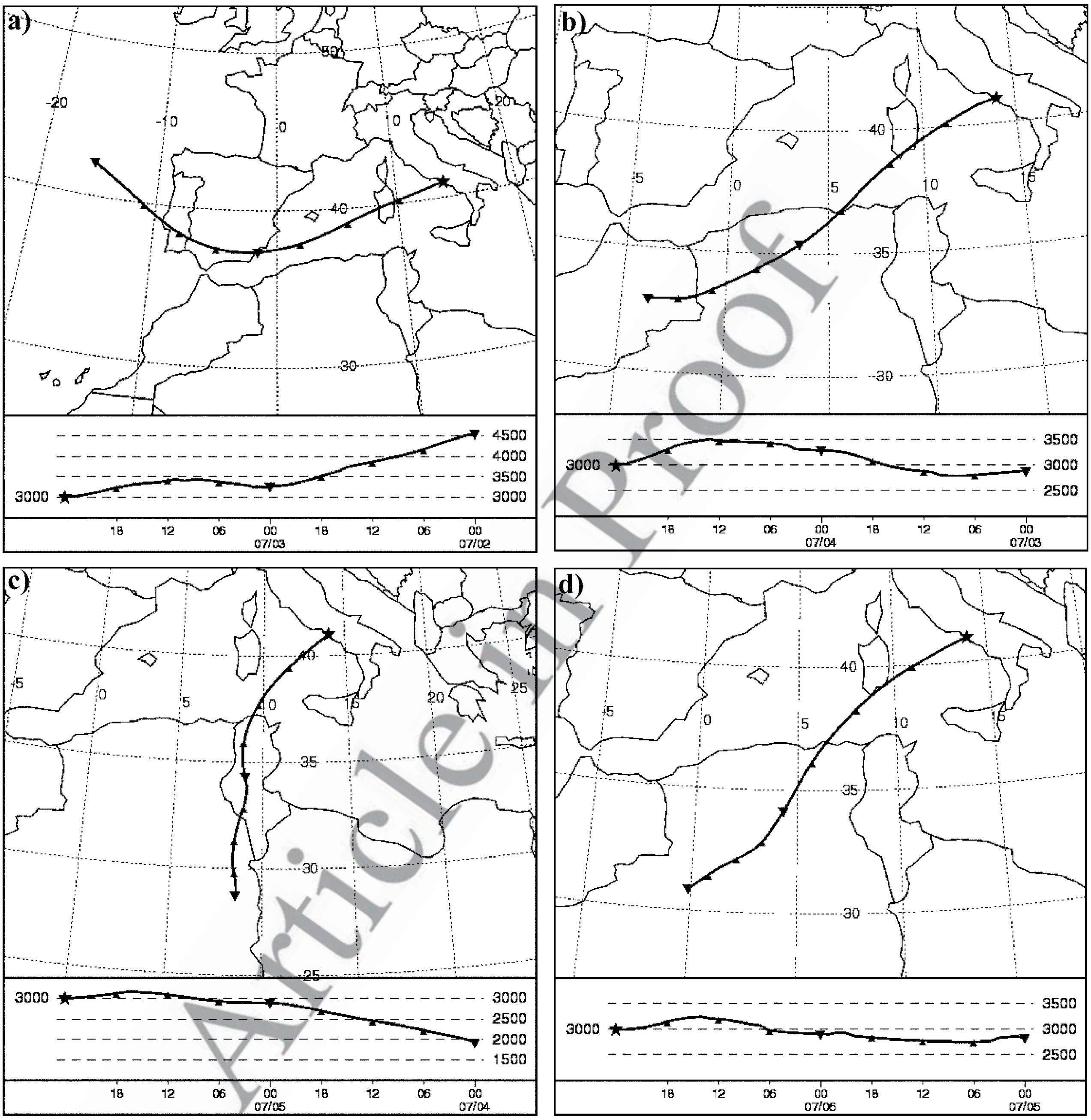

Figure 8. 24-hour backward trajectories for 4–10 July 1988 with the same start point in Italy (41°N, 14°E) at the altitude 3000 m: (a) 4 July, (b) 5 July, (c) 6 July, (d) 7 July, (e) 8 July, (f) 9 July, and (g) 10 July.

different. A deep low was situated in Ireland and Scotland with a strong trough emanating from it southward till latitude 30N and splitting the subtropical low into two separate cells. The eastern cell was centered on Sicily. Between the Irish low and this cell a strong southwesterly flow was formed from Mauritania across the western Mediterranean toward Italy and central Europe and even up to Scandinavia.

[31] The difference between the average flow for these five days and the average flow for all July days (Figure 7b) shows an almost similar situation to the flow itself. A closed low north of the Iberian Peninsula and a closed high centered south of the Italian Peninsula. Between them southerly flow was formed that crossed the northwestern Sahara. Its eastern flank reached central and northern Italy while the more western part crossed the Mediterranean and continued toward central and Western Europe.

[32] The results of the geopotential height investigation support the ones obtained from the investigation of the wind flow. The mean height in this period (Figure 7c) shows a deep low over Scotland with a well-defined trough due south along the European and the African coast, terminated at latitude 27N. A closed anticyclone, part of the subtropical high, was situated around Sicily. A steep gradient between

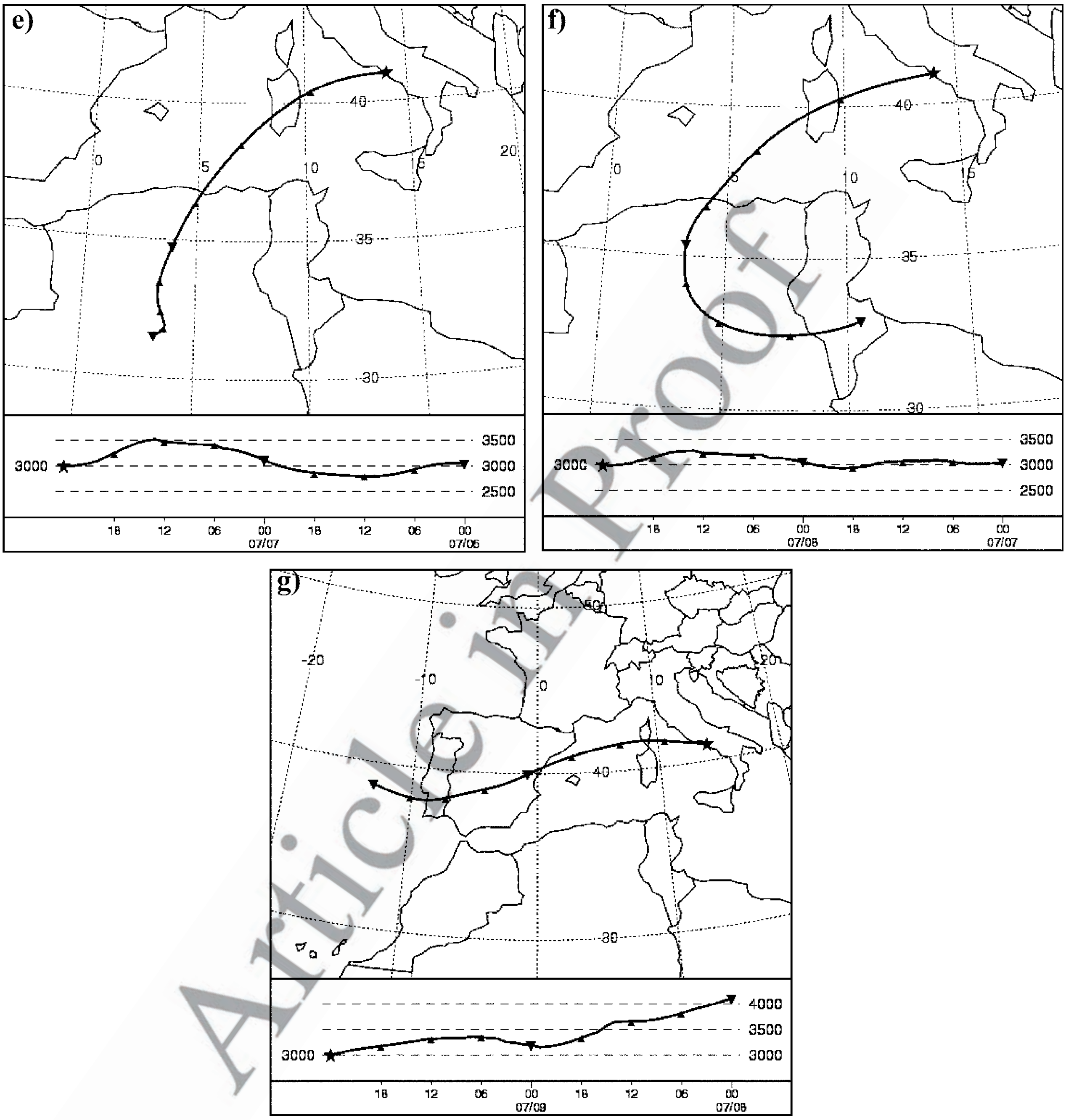

Figure 8. (continued)

these two systems suggests the existence of a strong southwestern flow through the Sahara toward Italy.

[33] The difference map (Figure 7d) shows a similar structure as the former but greatly enhanced: one can see a more then 80 m positive difference around southern Italy toward the Black Sea and a huge negative difference (140 m) centered around the British Islands. The mean July temperature (Figure 5a) shows a hot kernel in the northern Sahara and gradual cooling northward and southward. In the dusty period (Figure 7e), although the hottest area remains at the same place as in the monthly mean, a warm tong extends toward Italy the Adriatic and the Balkan. The peak difference (Figure 7f) of more then 8°C was observed east of the Adriatic. According to Figure 7a the warm desert flow reaches the eastern shores of the Adriatic, but it crosses northern and central Italy first. In the mean normal temperature distribution (Figure 7e) there was no difference between Italy and the eastern shore of the Adriatic. On the other hand, according to Figure 6 an area loaded with dust (AI = 2.1–2.4) was located in the northern Adriatic. It can be assumed therefore that the position of the peak difference is partly due to dust loading.

3.5.2. Back Trajectories

[34] Using the NOAA HYSPLIT model, we computed the trajectory of the wind, which presumably transported the dust into Italy, 72 hours backward for the period of the

dusty event, including one day before it started and two days after it ended. On 4 July (Figure 8a), before the beginning of the event, the trajectory had a west east direction, which excluded the possibility of dust transportation into Italy. On 5 July the trajectory direction became southwest northeast (Figure 8b) enabling the wind to tap the dust sources and transport the dust toward Italy. On the days 6–8 July the trajectory direction became approximately south north continuing to bring dust from the depth of the Sahara (Figures 8c–8e). On 9 July the trajectory still ended in Africa but near the Mediterranean coast in less dusty environment. Presumably, the sharp turn northward in the Algerian Sahara weakened the wind velocity and lessened its transportation ability (Figure 8f). On 10 July the trajectory became once more west east directed like before the beginning of the event and marked its end (Figure 8g).

3.5.3. Cases Measured by Lidar

[35] To give confidence to our results, concerning the average synoptic situation during TOMS-detected dust transportation toward Europe, we analyze the synoptics of some recent lidar-detected dust events in Rome (Italy) during 2001–2003. Measurements of dust loading by lidar were carried out in the July months of the years 2001, 2002 and 2003 in the outskirts of Rome (41.84°N, 12.64°E). Six cases with high dust loading were found as follows: 5, 6, and 9 July 2001 and 1, 2, and 9 July 2002 (G. P. Gobbi and F. Barnaba, personal communication, 2004). In addition, we looked into the AERONET data in Rome and in Oristano (39.9°N, 8.5°E): aerosol optical thickness (AOT) at the 440 nm. The AOT values for the selected six days were above the monthly average, while for other (non dusty) days they were well below it. Therefore both the AERONET data and the lidar measurements showed that the days selected for the synoptic analysis were dusty. The composite patterns of atmospheric variables for the selected six days were examined in the same way as for the previous case study. The results for lidar-detected dust episodes were found to be mainly similar to the results based on the TOMS data (Figure 9), although the absolute values of the height and temperature difference are smaller. This similarity in the average synoptic situations for the dust transportation events over Europe, detected with the aid of three different approaches at different times, is significant, and enhances the credibility of our results.

3.6. Transportation of Dust North of the Alps

[36] The results of the above investigation of the dust transport into Italy with the right synoptic situation, hinted to the possibility, that in extreme cases the transported dust can reach the central European planes north of the Alps, even up to the shores of the Baltic. As was mentioned above, Saharan dust was found on the Jungrfraujoch at the middle of the Alps [*Collaud Coen et al.*, 2003]. Consequently we looked once more into the data of the 14 months of July in the area (45°–50°N, 5°–15°E). We assumed that due to the great quantity of pollution in this area only high AI values would indicate presence of dust in reasonable quantities. So, besides the cases with AI equal or greater then one standard deviation, we also looked for cases with AI greater then two standard deviations. Although we found 20 cases with AI greater then one standard deviation, the spatial distribution of the AI showed isolated high-AI areas indicating pollution more then dust. Only two days, 27 and 28 July 1983, were found with AI greater then two standard deviations. Additionally, the spatial distribution of the AI in these days showed a continuous high-AI area, from the Mediterranean up to the shore of the Baltic. Consequently, we decided to investigate the synoptic situation of these days as a case study.

3.6.1. Wind Flow

[37] Comparing between the wind flow pattern in this case (Figure 10a) with these of the average wind flow at the dusty cases in Italy (Figure 3b) and at the extremely dusty period in 5–9 July 1988 (Figure 7a), we can see an increase of the synoptic activity in the North Eastern Atlantic. In the dusty cases out of all the cases a trough existed along the European and African coast of the Atlantic between the two cells of the Subtropical High. This trough was enhanced and terminated more to the south in the case of the extremely dusty period. Consequently the southwestern flow in the forward-eastern flank of the trough was sufficient to transport dust toward the western Mediterranean but no more to the north. The situation on 27–28 July was quite different due to considerably higher synoptic activity in the Northern Atlantic. The western high-pressure cell intensified and moved to the northeast. The eastern cell moved also northward. The low between them, on the contrary, moved more to the south, to the Bay of Biscay. The trough emanating from this low southward reached more to the south and was terminated only at the 25°N parallel. Its axis was situated more to the east compared to the previous cases, touching the African coast. This situation enabled the existence of a long, continuous and efficient flow from the dust source areas in the Western Sahara toward central Europe.

3.6.2. Geopotential Height

[38] The picture supplied by the geopotential height (Figure 10b) is actually identical to the wind flow, even enhancing it.

3.6.3. Temperature

[39] The average temperature map for these days shows a well-defined warm pocket emanating from the hot kernel in the Sahara northward into Europe (Figure 10c). The difference between these two days and the multiyear average shows a warming of up to 7 degrees in Europe relative to the average (Figure 10d). The question we asked already is, whether this warming is caused by the warm southerly flow, by the subsidence in the anticyclone in Europe or by the dust in the atmosphere. Although we have no clear answer to this problem, we think that to all the three has part in it.

3.6.4. Trajectories

[40] The back trajectories started on the 27 July (Figure 10e) and on 28 July (Figure 10f) both show clearly the possibility to transport dust from the source areas in the Sahara into Europe. It also shows that in the source area the dust was near the ground but it reached Europe at the height of 3000 m. indicating active atmospheric processes along the route.

4. Conclusions

[41] TOMS-AI data over Italy and vicinity (36°N–46°N, 10°E–18°E), and data of climatological variables (wind, geopotential height and temperature) at the 700 hPa level

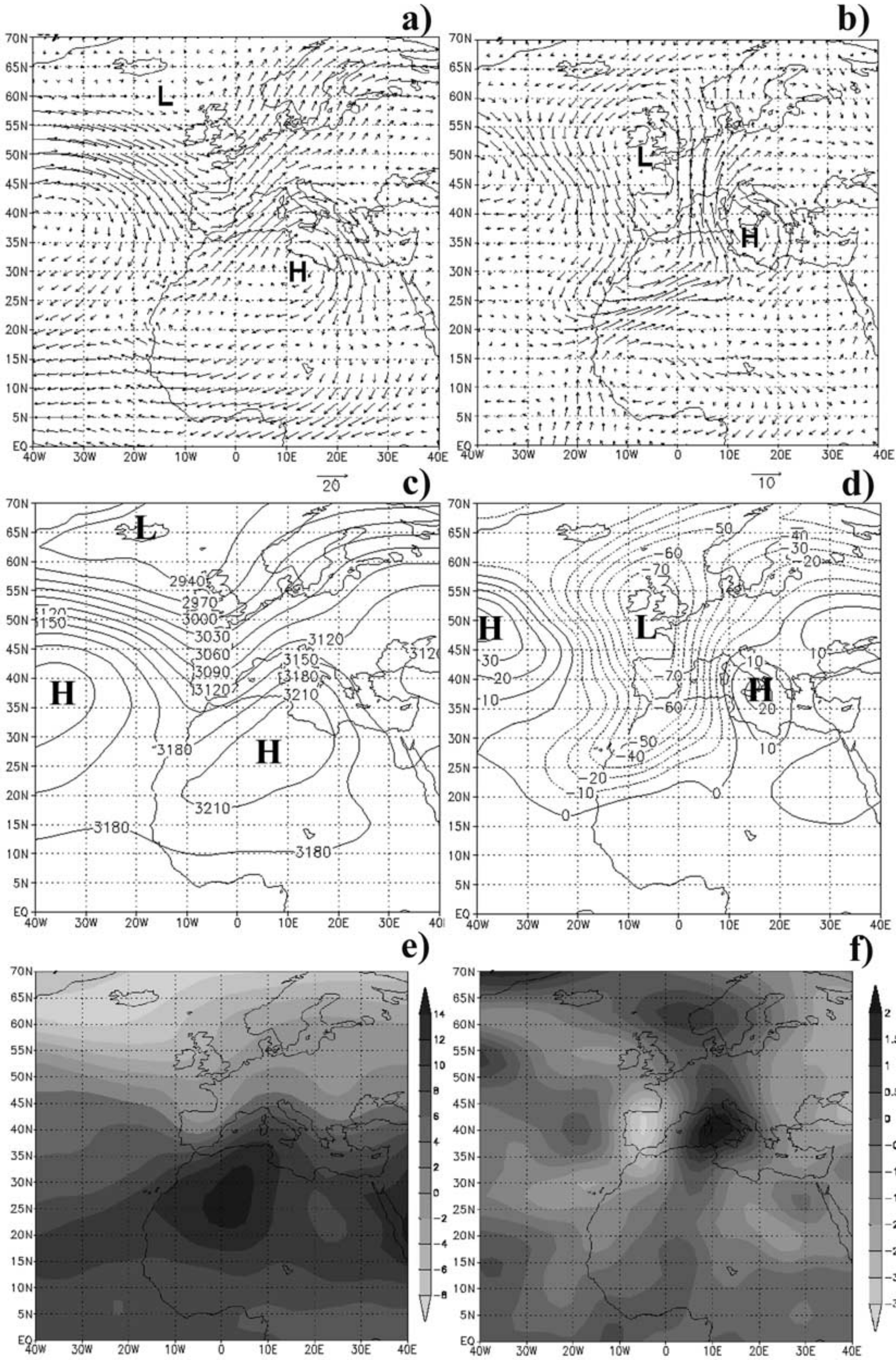

Figure 9. Mean maps obtained by lidar measurements in high dust load days: 5, 6, and 9 July 2001 and 1, 2, and 9 July 2002. (a) Average wind flow of the dusty cases at 700 hPa. (b) Average wind flow difference, that is, dusty cases minus all the cases. (c) Average geopotential height of the dusty cases at 700 hPa. (d) Average geopotential height difference, that is, dusty cases minus all the cases. (e) Average temperature of the dusty cases at 700 hPa. (f) Average temperature difference, that is, dusty cases minus all the cases.

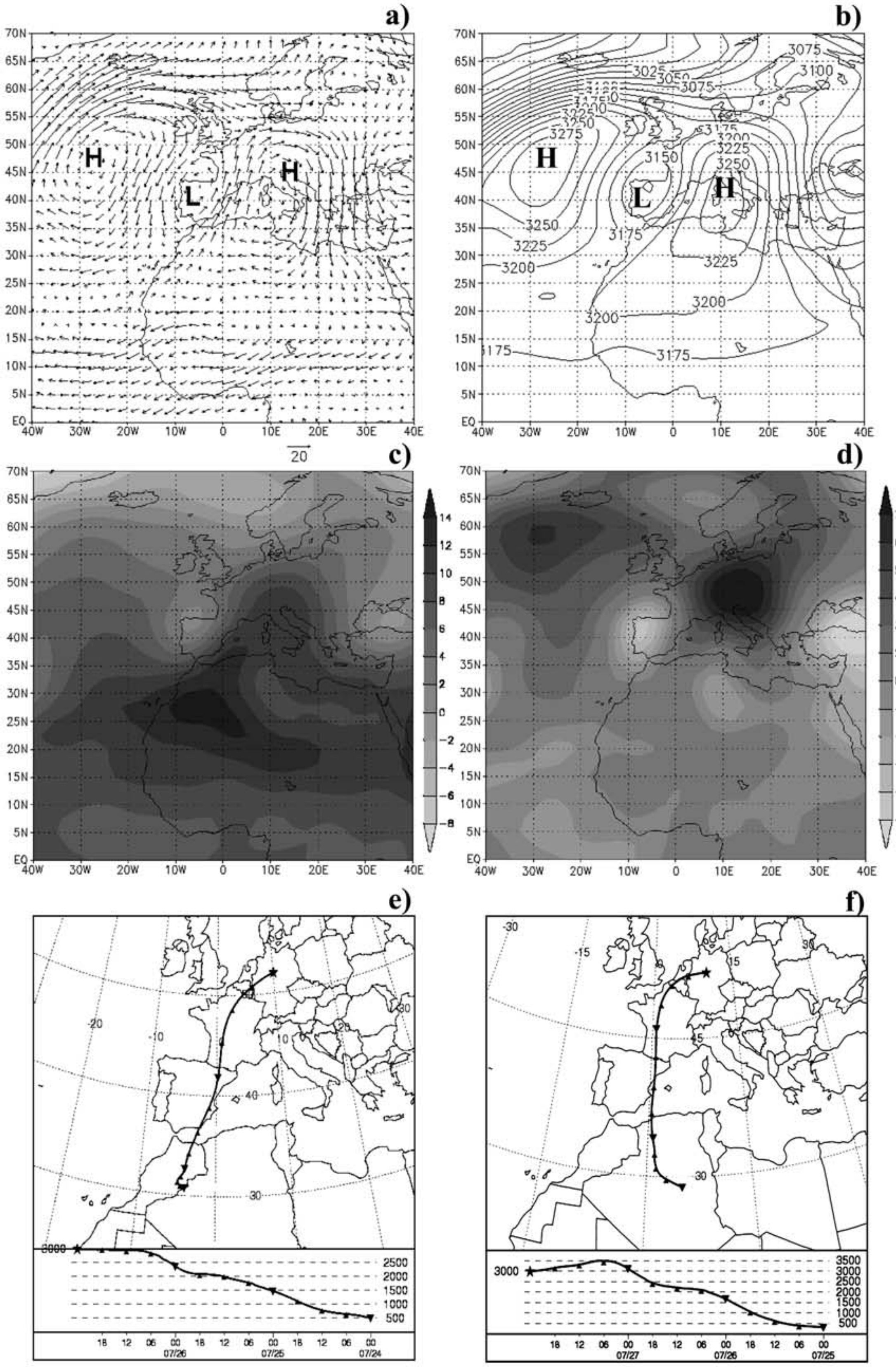

Figure 10. Mean maps of atmospheric variables of a case of dust transportation into central and northern Europe, 27–28 July 1983: (a) mean wind flow, (b) mean geopotential height, (c) mean temperature, (d) temperature difference between the two dusty days and the monthly average, (e) back trajectory for 27 July 1983, and (f) back trajectory for 28 July 1983.

from the area (0–70°N, 40°W–40°E) were extracted for the July months for the period 1979–1992. Days with AI ≥ of one standard deviation above the July average of every single year were defined as dusty. Average of the climatological variables during the dusty cases were compared with the average of all the cases. The differences in the synoptic situation between the general and the dusty cases were analyzed. This enabled to detect the most frequent directions from were the dust was transported into Italy. A case study, based on the same technique as for the average cases, was carried out for a 5 day dusty period.

[42] Significant differences between the normal and the dusty synoptic situations were identified in wind flow, in geopotential height and in temperature. The two main features that influence the transportation of dust from Africa into Europe and particularly into Italy is the trough that emanates from the Icelandic low southward, and the subtropical high. The strength and the position of these two systems define if dust transportation will occur, its direction and its efficiency. In the cases of dust outbreaks into Europe, the trough emanating from the Icelandic Low is prominent with its axis quite to the east crossing the Iberian Peninsula and in the south close to the African coast. The eastern cell of the subtropical high is considerably more eastern, northern and stronger. The steep gradient between them causes a strong southwesterly flow capable of transporting dust toward Italy. The closeness of the subtropical high to, and the strong southwestern flow aimed at the Italian Peninsula in the dusty period are associated with the strong warming over Italy in these days. However, we assume that partially it is because of the diabatic heating caused by the presence of the dust. Alternatively, when no transportation occurs, the Icelandic Low is separated from the lower latitudes by a strong lateral flow. There is no trough southward or a very weak one. The subtropical high is also weak. Its eastern cell is positioned quite to the south and the west and weak, while the center of the western cell located far to the west. These conditions are similar but greatly enhanced during the periods of the case studies. Analysis of back trajectories for the case study supports the results of our synoptic analysis.

[43] As mentioned in section 1, dust affects significantly the synoptic systems by cooling the surface and altering the atmospheric thermal structure and cloud microphysics. In this connection, better understanding of the synoptic situation may help to improve the dust packages in atmospheric models. The significance of the findings, obtained in the current study, consists in defining the mean synoptic situation during the Saharan dust transportation over the Mediterranean into Southern Europe, which could help in accurate prediction of dust events, with application to a wide range of topics like weather forecasts, traffic safety, agriculture, marine biology, health problems, etc.

[44] **Acknowledgments.** This study was supported by the EU DETECT project (contract EVK2-CY-1999-00048) and by GLOWA–Jordan River from the Israeli Ministry of Science and Technology and the German Bundesministerium für Bildung und Forschung (BMBF). Special thanks to Melina Dayan for her help with the data processing and the graphics.

References

Alpert, P., and E. Ganor (1993), A jet stream associated heavy dust storm in the western Mediterranean, *J. Geophys. Res.*, *98*(D4), 7339–7349.

Alpert, P., and B. Ziv (1989), The sharav cyclone: Observations and some theoretical considerations, *J. Geophys. Res.*, *94*(D15), 18,495–18,514.

Alpert, P., Y. J. Kaufman, Y. Shai-El, D. Tanre, A. da-Silva, S. Schubert, and J. H. Joseph (1998), Quantification of dust forced heating of the lower troposphere, *Nature*, *395*, 364–370.

Alpert, P., P. Kishcha, A. Shivelman, S. O. Krichak, and J. H. Joseph (2004), Vertical distribution of Saharan dust based on 2.5-year model predictions, *Atmos. Res.*, *70*, 109–130.

Avila, A., J. Querall, F. Gallart, and J. M. Vide (1996), African dust over northeastern Spain: Mineralogy and source regions, in *The Impact of Desert Dust Across the Mediterranean*, edited by S. Guerzoni and R. Chester, pp. 201–205, Springer, New York.

Barkan, J., H. Kutiel, P. Alpert, and P. Kishcha (2004a), The synoptics of dust intrusion days from the African continent into the Atlantic Ocean, *J. Geophys. Res.*, *109*, D08201, doi:10.1029/2003JD004416.

Barkan, J., H. Kutiel, and P. Alpert (2004b), Climatology of dust sources over the North African region, based on TOMS data, *Indoor Built Environ.*, *13*, 407–419.

Bonelli, P., and G. M. B. Marcazzan (1996), Elemental composition and air trajectories of African dust transported in northern Italy, in *The Impact of Desert Dust Across the Mediterranean*, edited by S. Guerzoni and R. Chester, pp. 275–283, Springer, New York.

Carlson, T. N., and J. M. Prospero (1972), The large-scale movement of Saharan air outbreaks over the northern equatorial Atlantic, *J. Appl. Meteorol.*, *11*, 283–297.

Collaud Coen, M., E. Weingarten, D. Schaub, C. Hueglin, C. Corrigan, M. Schwikowski, and U. Baltenspreger (2003), Saharan dust events at the Jungfraujoch: Detection by wavelength dependence of the single scattering albedo and analysis of the events during the years 2001 and 2002, *Atmos. Chem. Phys. Discuss.*, *3*, 5547–5594.

Conte, M., M. Colarino, and F. Piervitali (1996), Atlantic disturbances deeply penetrating the African continent: Effects over Saharan regions and the Mediterranean basin, in *The Impact of Desert Dust Across the Mediterranean*, edited by S. Guerzoni and R. Chester, pp. 93–102, Springer, New York.

Dayan, U., J. Hefter, J. Miller, and G. Gutman (1991), Dust intrusion events into the Mediterranean basin, *J. Appl. Meteorol.*, *30*, 1185–1199.

Di Sarra, A., T. Di Iorio, M. Cacciani, G. Fiocco, and D. Fua (2001), Saharan dust profiles measured by lidar at Lampedusa, *J. Geophys. Res.*, *106*, 10,335–10,347.

Dulac, F., C. Moulin, C. E. Lambert, F. Guillard, J. Poitou, W. Guelle, C. R. Quetel, X. Schneider, and U. Ezal (1996), Quantitative remote sensing of African dust transport in the Mediterranean, in *The Impact of Desert Dust Across the Mediterranean*, edited by S. Guerzoni and R. Chester, pp. 25–49, Springer, New York.

Egger, J., P. Alpert, A. Taffner, and B. Ziv (1995), Numerical experiments on the genesis of sharav cyclones, *Tellus, Ser. A*, *47*, 162–174.

Gobbi, G. P., F. Barnaba, R. Giorgi, and A. Santacasa (2000), Altitude-resolved properties of a Saharan dust event over the Mediterranean, *Atmos. Environ.*, *34*, 5119–5127.

Hamonou, E., P. Chazette, D. Bali, F. Dulac, X. Schneider, F. Galani, G. Ancellet, and A. Papayanis (1999), Characterization of the vertical structure of the Saharan dust transport to the Mediterranean basin, *J. Geophys. Res.*, *104*(D22), 256–270.

Herman, J. R., and E. Celarier (1997), Earth surface reflectivity climatology at 340–380 nm from TOMS data, *J. Geophys. Res.*, *102*(D23), 28,003–28,011.

Israelevich, P. L., Z. Levin, J. H. Joseph, and E. Ganor (2002), Desert aerosol transport in the Mediterranean region as inferred from the TOMS aerosol index, *J. Geophys. Res.*, *107*(D21), 4572, doi:10.1029/2001JD002011.

Karayampudi, M. V., et al. (1999), Validation of the Saharan dust plume conceptual model using lidar, Meteosat, and ECMWF data, *Bull. Am. Meteorol. Soc.*, *80*(6), 1045–1075.

Kaufman, Y. J., D. Tanre, and O. Boucher (2002), A satellite view of aerosols in the climate system, *Nature*, *419*, 215–233.

Kishcha, P., F. Barnaba, G. P. Gobbi, P. Alpert, A. Shtivelman, S. O. Krichak, and J. H. Joseph (2004), Vertical distribution of Saharan dust over Rome (Italy): Comparison between 3-year model predictions and lidar soundings, *J. Geophys. Res.*, doi:10.1029/2004JD005480, in press.

Koren, I., J. H. Joseph, and P. L. Israelevich (2003), Detection of dust plumes and their sources in northeastern Libya, *Can. J. Remote Sens.*, *29*(6), 792–796.

Lenes, J. M., et al. (2001), Iron fertilization and the Trichodesmium response on the west Florida shelf, *Limnol. Oceanogr.*, *46*(6), 1261–1277.

Moulin, C., C. E. Lambert, U. Dayan, M. Ramonet, P. Bouquet, M. Legrand, Y. J. Balkansky, W. Guelle, B. Marticorena, and F. Dulac (1998), Satellite climatology of African dust transport in the Mediterranean atmosphere, *J. Geophys. Res.*, *103*(D11), 13,137–13,144.

Prodi, F., and G. Fea (1979), A case of transport and deposition of Saharan dust over the Italian peninsula and southern Europe, *J. Geophys. Res.*, *84*(C11), 6951–6960.
Prospero, J. M. (1996), Saharan dust transport over the North Atlantic Ocean and the Mediterranean, in *The Impact of Desert Dust Across the Mediterranean*, edited by S. Guerzoni and R. Chester, pp. 133–151, Springer, New York.
Prospero, J. M., P. O. Ginoux, S. Torres, E. Nicholson, and T. E. Gill (2002), Environmental characterization of global sources of atmospheric soil dust identified with the NIMBUS 7 Total Ozone Mapping Spectrometer (TOMS) absorbing aerosol product, *Rev. Geophys.*, *40*(1), 1002, doi:10.1029/2000RG000095.
Rosenfeld, D., Y. Rudich, and R. Lahav (2002), Desert dust suppressing precipitation: A possible desertification loop, *Proc. Natl. Acad. Sci. U. S. A.*, *98*, 5975–5980.
Stidd, C. K. (1956), The use of correction fields in relating precipitation in circulation, *J. Meteorol.*, *11*, 202–213.
Swap, R. M., M. Garstang, S. Greco, R. Talbot, and P. Kallberg (1992), Saharan dust in the Amazon basin, *Tellus, Ser. B*, *44*, 133–149.
Torres, O., P. K. Bhartia, J. R. Herman, A. Sinyuk, P. Ginoux, and B. A. Holben (2002), A long term record of aerosol optical depth from TOMS observations and comparison to AERONET measurements, *J. Atmos. Sci.*, *59*, 398–413.
Walsh, J. J., and K. A. Steidinger (2001), Saharan dust and Florida red tides: The cyanopite connection, *J. Geophys. Res.*, *106*(C6), 11,597–11,612.
Washington, R., M. Todd, N. J. Middleton, and A. S. Goudie (2000), Dust storm source areas determined by the Total Ozone Monitoring Spectrometer and surface observations, *Ann. Assoc. Am. Geogr.*, *93*(2), 297–313.
Westphal, D. L., O. B. Toon, and T. N. Carlson (1987), A two dimensional numerical investigation of the dynamics and microphysics of Saharan dust storms, *J. Geophys. Res.*, *92*(D3), 3027–3049.

P. Alpert, J. Barkan, and P. Kishcha, Dept. of Geophysics and Planetary Sciences, Faculty of Exact Sciences, Tel-Aviv University, Ramat Aviv, Tel-Aviv, 69978, Israel. (yossib@vortex.tau.ac.il)
H. Kutiel, Dept. of Geography, University of Haifa, Haifa 31999, Israel. (kutiel@geo.haifa.ac.il)